Bioprocess Biosyst Eng (2015) 38:1773–1781
DOI 10.1007/s00449-015-1418-3

ORIGINAL PAPER

Biosynthesis of silver nanoparticles and its antibacterial and antifungal activities towards Gram-positive, Gram-negative bacterial strains and different species of *Candida* fungus

Rahisuddin[1] · Shaeel Ahmed AL-Thabaiti[2] · Zaheer Khan[2] · Nikhat Manzoor[3]

Received: 1 January 2015 / Accepted: 18 May 2015 / Published online: 28 May 2015

Abstract Biomimetic and economic method for the synthesis of silver nanoparticles (AgNPs) with controlled size has been reported in presence of shape-directing cetlytrimethylammonium bromide (CTAB). Biochemical reduction of Ag^+ ions in micellar solution with an aqueous lemon extract produced spherical and polyhedral AgNPs with size ranging from 15 to 30 nm. The influence of [CTAB] and [lemon extract] on the size of particles, fraction of metallic silver and their antimicrobial properties is discussed. The AgNPs were evaluated for their antimicrobial activities (antibacterial and antifungal) against different pathogenic organisms. For this purpose, AgNPs were tested against two model bacteria (*Staphylococcus aureus* (MTCC3160) and *Escherichia coli* (MTCC405)) and three species of *Candida* fungus (*Candida albicans* (ATCC90028), *Candida glabrata* (ATCC90030) and *Candida tropicalis* (ATCC750). AgNPs were found to be highly toxic towards both bacteria. The inhibition action was due to the structural changes in the protein cell wall.

Keywords Antimicrobial activity · Biosynthesis · Nanoparticles · *Candida* fungus

✉ Rahisuddin
rahisuddin@jmi.ac.in

[1] Department of Chemistry, Jamia Millia Islamia (Central University), New Delhi 110025, India

[2] Department of Chemistry, Faculty of Science, King Abdulaziz University, P.O. Box 80203, Jeddah 21589, Saudi Arabia

[3] Department of Medical Laboratories Technology, Taibah University, P.O. Box 344, Madinah 30001, Kingdom of Saudi Arabia

Introduction

Silver has been used for thousands of years for ornaments, medicine, food, textile, photography, electronics, dental fillings and utensils. Silver and its nanoparticles have been used as an antimicrobial in a variety of industrial, healthcare and domestic applications [1]. Silver inhibits the growth of bacteria and fungi on clothing, such as socks. It is added to reduce odours and the risk of bacterial and fungal infections [2]. Nowack et al. investigated the behaviour of nine silver-containing fabrics under conditions relevant to washing. They also determined the amount and the form of silver released during washing [3]. The silver ion, Ag^+, is bioactive and in sufficient concentration readily kills bacteria in vitro. Exposure to silver nanoparticles has been associated with inflammatory, oxidative, genotoxic and cytotoxic consequences. The silver particulates primarily accumulate in the liver, but have also been shown to be toxic in other organs including the brain. Nano silver applied to tissue-cultured human cells leads to the formation of free radicals, raising concerns of potential health risks [4, 5]. Metallic silver in its various oxidation states has long been recognized as having an inhibitory effect towards many bacterial strains and microorganisms [6]. Due to their wide applications, three broad categories of synthetic routes (physical vapour deposition, ion implantation, or wet chemistry) have been used by various researchers from three decades in the presence and absence of soft and hard templates [7–15]. Bakshi in his pioneering feature article proposed that metal nanoparticles would be acted as model air pollutants with a strong tendency for pulmonary surfactants (surface-active and shape-directing stabilizing and/or capping agents) which help to understand their potential threat to the human respiratory system in relation to nanotoxicology [16]. Generally, a cationic

surfactant, CTAB as a dispersant raised much interest for preparing shape-control (from nanospherical, nanorods, nanocubes, nanotriangle, nanotubes, etc.) AgNPs [17–21]. Yu et al. reported [22] a modified silver mirror reaction method for the synthesis of advanced nano silver having various morphologies by adjusting the concentrations of CTAB and the Tollens' reagent, and the uses of CTAB mainly considered as template or capping agents to form controllable shape and protect the product from agglomeration.

It has been established that silver and its nanomaterials have been found to exhibit interesting antibacterial activities [23–27] and these biocompatible inert nanomaterials also have potential applications in cancer diagnosis and therapy [28, 29]. In the biosynthesis of nanoparticles, the microbial enzymes and the plant phytochemicals (ascorbic acid, flavonoids, tannins, terpenoids and polyhydroxy phenols) with antioxidant or reducing properties have been responsible for reduction of metal compounds into their respective nanoparticles [30–32]. The literature contains abundant reports aimed at understanding the role of biomolecules in the extracellular green synthesis of AgNPs. The resulting nanoparticles have mixed morphology (spherical, triangular, truncated triangular nanoplates, nanorods, tetrahedral, hexahedral and irregular) due to the presence of various natural biomolecules and/or others constituents. To avoid toxic chemicals, a new field of study has been developed for a clean, reliable, biocompatible, benign and eco-friendly process to synthesize nanoparticles. Lemon juice has been used by humans in the preparation of a wide variety of foods, drinks and cocktails. It has been established that lemon juice contains various vitamins (ascorbic acid, thiamine, niacin, riboflavin), citric acid, flavonones (rutin, luteolin, hesperidin, naringin, etc.), phenolic compounds in the form of glycosides and minerals in varying quantities [33–35]. Out of these chemical constituents, lemon juice is the rich source of citric acid, ascorbic acid and minerals [36, 37]. It contains significant concentrations of ascorbic acid and citric acid (ca. 47 g/l in the juices), which give lemons a sour taste [38]. Lemon oil is also used as a nontoxic insecticide agent, which does not influence the human immune system. The chemical structures of the main constituents of lemon juice are given in Scheme 1.

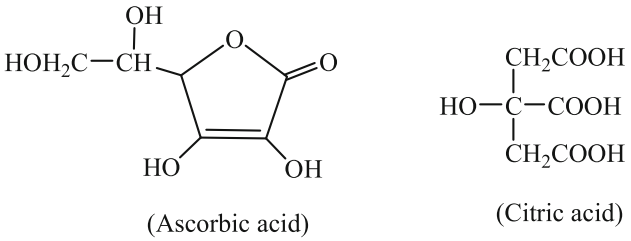

Scheme 1 Main chemical constituents of lemon aqueous extract

The low pH of juice makes it antibacterial. Prathna and his coworkers synthesized AgNPs at room temperature by treating silver ions with the lemon extract in the presence and absence of sunlight [39, 40]. Nisha et al. [41] and Vankar and Shukla [42] described the synthesis and antidermatophytic and antimicrobial applications of AgNPs using an aqueous extract of lemon peels and leaves, respectively, and suggested that the extract acted as a reducing and encapsulating agent [42]. Recently, we have reported a simple method for the synthesis of lemon aqueous extract-assisted bioconjugated AgNPs [43]. Till date, there are no reports on the microbial activities of AgNPs using citrus lemon aqueous juice as reducing agent. In this paper, we report the antimicrobial activities of lemon juice-directed synthesis of AgNPs in aqueous media. For this purpose, two bacteria (*Staphylococcus aureus* and *Escherichia coli*) and three species of *Candida* fungus (*Candida albicans*, *Candida glabrata* and *Candida tropicalis*) were chosen.

Experimental

Chemicals

$AgNO_3$ and CTAB were purchased from Sigma-Aldrich and used without further purification. The 10 g fresh lemons were collected from the local market near the Jamia Millia Islamia campus, New Delhi, India. All the solutions were prepared using deionized double-distilled water. Microorganisms used in this study were as follows: Gram-positive bacteria, *S. aureus* (MTCC3160); Gram-negative bacteria, *E. coli* (MTCC405); fungus, *C. albicans* (ATCC90028); *C. glabrata* (ATCC90030) and *C. tropicalis* (ATCC750) were used as received. Luria broth (microbiology grade) media was used for the determination of minimum inhibitory concentration (MIC). Bacteria were incubated at 37 °C and shaken in a thermostat.

Preparation and characterization of AgNPs

10.0 g of lemons was peeled, rinsed with deionized water, chopped into four pieces, added to 250 cm^3 deionized water, heated on a water bath at 60 °C for 30 min, and allowed to cool and stand for 24 h at room temperature. The resulting solution was filtered through Whatman No. 1 filter paper to collect a perfect white transparent lemon aqueous extract solution. The titrimetry method was used to determine the concentrations of citric acid and ascorbic acid, bioreductants, in our lemon fruit samples. A series of titrations was carried out with sodium hydroxide and iodine solution using phenolphthalein (appearance of a pale pink colour; end point) and starch (appearance of a blue black

colour; end point) as an indicator, respectively, for citric and ascorbic acids [44]. Our lemon samples contained ca. 2.5 % citric acid and ca. 0.7 % ascorbic acid. These concentrations were in good agreement with the results of Prathna et al. [39]. The extracts thus obtained were used directly for the preparation of AgNPs and also for the assessment of antimicrobial potential through various chemical assays. AgNPs were synthesized by the bioreduction of Ag^+ ions with aqueous lemon extract in the absence and presence of micellar CTAB solution. The initial experiments show that the reaction mixture ($AgNO_3$; 3.0×10^{-3} mol/dm^3 + lemon extract; from 2.0 to 0.5 cm^3) turned yellowish milky as the reaction time increases. So the shape-directing CTAB aqueous solution (from 0.4 to 1.0×10^{-4} mol/dm^3) was added to obtain a clear and perfect transparent coloured solution of AgNPs [8, 9] to prevent the unlimited growth of nanoparticles and/or precipitation. The transparent colourless solution was converted to the characteristic pale yellow and orange-red colour, when CTAB was used as a stabilizing agent. Reduction was initiated several minutes after the addition of the lemon extract at room temperature (25 °C). UV–Vis absorption spectra of the resulting AgNPs were acquired using UV–visible spectrophotometer, UV-260 Shimadzu, with 1 cm^3 quartz cuvette and transmission electron microscope (JEOL, JEM-1011; Japan) to monitor the morphology of AgNPs. To determine the interaction of the AgNPs with bacteria and fungus, the coloured solution of AgNPs was homogenized with a Fisher Bioblock Scientific ultrasonic cleaning container for 10 min at room temperature.

Antibacterial and antifungal assay of AgNPs

The antimicrobial susceptibility of AgNPs was evaluated using the disc diffusion or Kirby–Bauer method [45]. Zones of inhibition were measured after 24 h of incubation at 35 °C. The standard dilution micro method for determining the minimum inhibitory concentration (MIC) leading to the inhibition of bacterial growth was performed. In a typical experiment, MIC was determined as the lowest concentration that inhibited the visible growth of the used

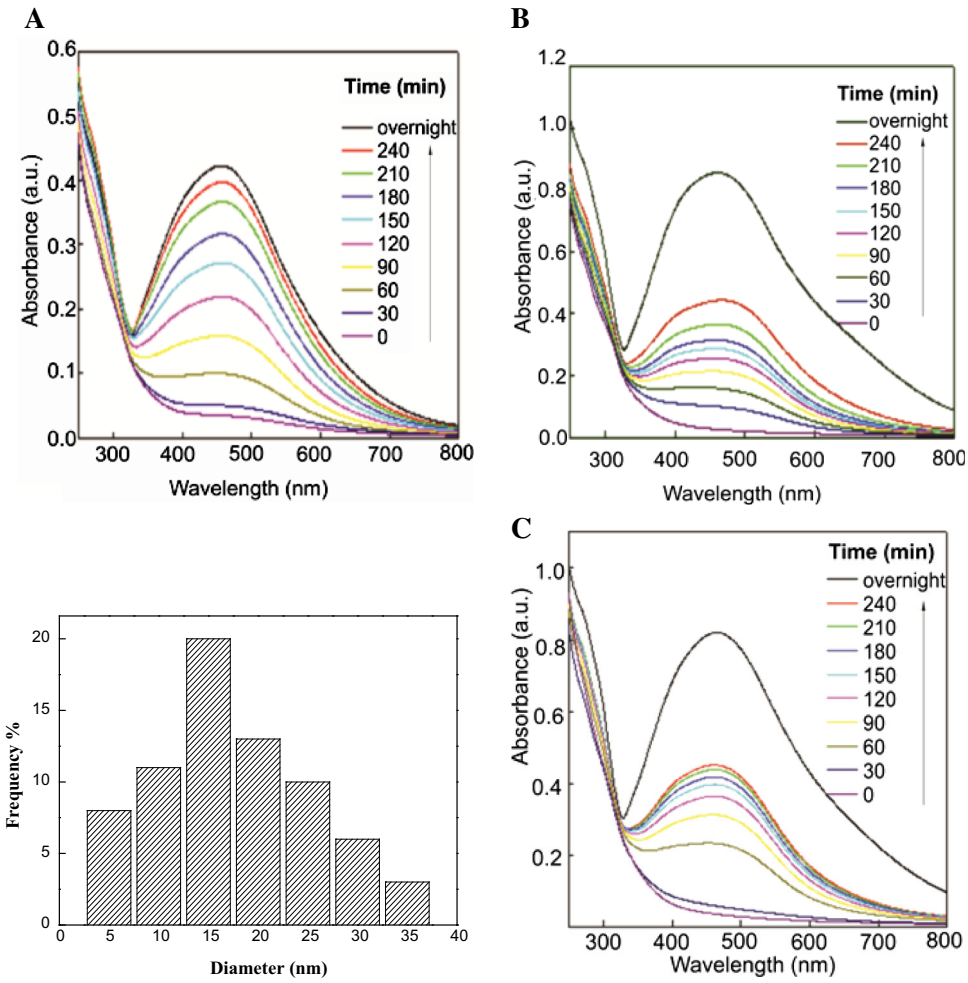

Fig. 1 Effect of [CTAB] on UV–Vis. spectra and bioreduction kinetics for the formation of CTAB-stabilized AgNPs. Reaction conditions: $[Ag^+] = 3.0 \times 10^{-3}$, [lemon extract] = 0.5 cm^3, [CTAB] = 0.4 (**a**), 0.8 (**b**) and 1.0×10^{-4} mol dm^{-3} (**c**)

bacterium. The presence of a clear zone around the circular disc on the plate medium containing different concentrations of AgNPs was recorded as inhibition against the microbial species. The stability of discs containing standard antibiotic (gentamicin) and antifungal (fluconazole) drugs was compared with regard to antibacterial and antifungal activities, respectively. The reference solution (water taken after the last dialysis) did not show antimicrobial activities. Free Ag^{+} ions in the form of $AgNO_3$ cultured under the same conditions were used as a control.

Results and discussion

Morphology and [CTAB] effect on the growth of AgNPs

To find out the preliminary information about the morphology of AgNPs, UV–visible absorption spectra of pale yellow–brown silver sols were recorded at different time intervals as well as for three different [CTAB] values which showed a well-defined surface plasmon absorption band with a maximum of 450, 470 and 475 nm for 0.4, 0.8 and 1.0×10^{-4} mol dm^{-3} [CTAB], respectively, characteristic of nanosized spherical or roughly spherical AgNPs (Fig. 1). With increase in [CTAB], the peak shifted to a higher wavelength (redshift) and the width of the absorption band was also increased, suggesting the shape-directing role of the CTAB surfactant. Interestingly, there was a gradual change in the spectrum and shape of SRP band shifted with [CTAB] (Fig. 1). The shape of the absorption band gradually became broad with a wide bandwidth and exhibited a systematic redshift of total 25 nm at higher [CTAB]. The shifting of wavelength might be due to anisotropic growth and multiplasmon excitation of facted AgNPs [46]. CTAB sub- and post-micellar aggregates formed an ion pair with the lone pairs of –OH group electrons of active constituents of lemon extract, i.e., citric

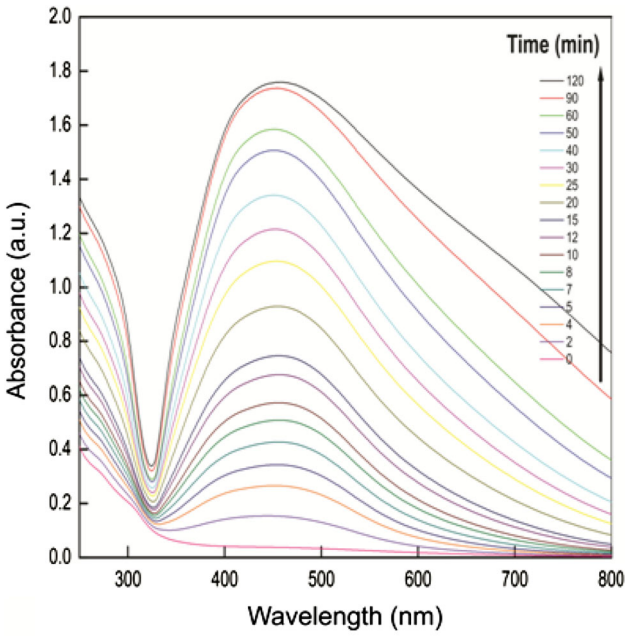

Fig. 2 Effect of sun light on the growth and bioreduction kinetics for the formation of CTAB-stabilized AgNPs. Reaction conditions: $[Ag^{+}] = 3.0 \times 10^{-3}$, [CTAB] $= 0.6 \times 10^{-4}$ mol dm^{-3}, [lemon extract] $= 0.4$ cm^3

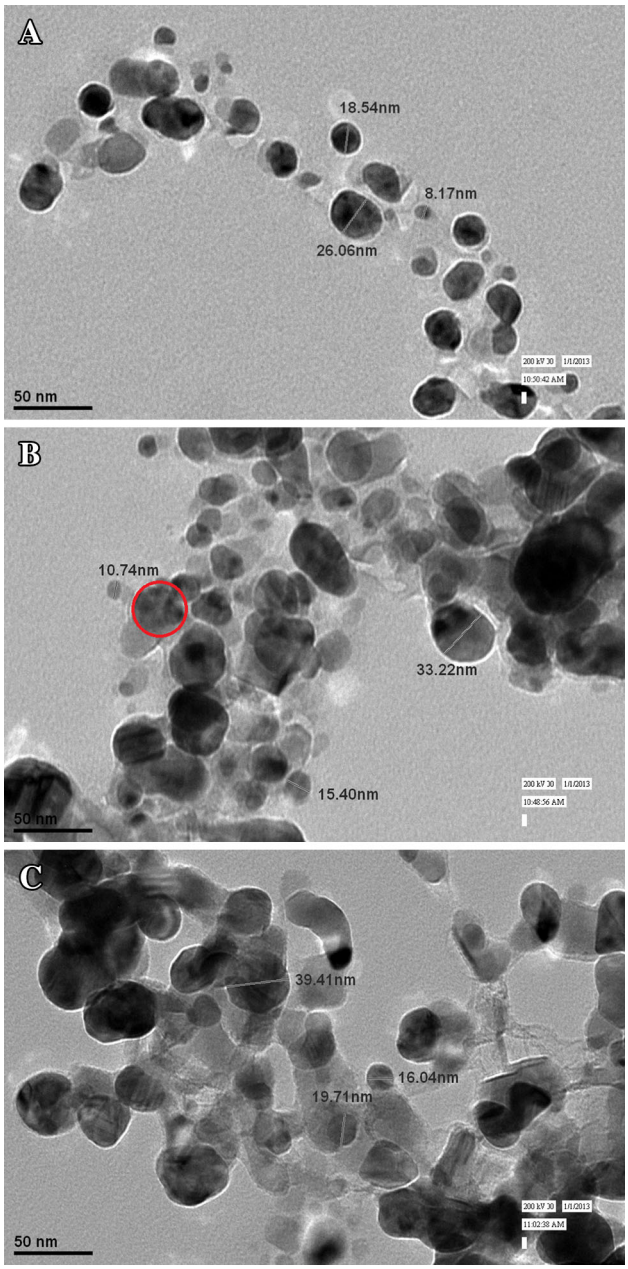

Fig. 3 TEM images of AgNPs. Reaction conditions: $[Ag^{+}] = 3.0 \times 10^{-3}$, [lemon extract] $= 0.5$ cm^3, [CTAB] $= 0.4$ (**a**), 0.6 (**b**) and 0.8×10^{-4} mol dm^{-3} (**c**)

and ascorbic acids. As a result, both reactants may be assumed to be totally present in the Stern layer (most of the ionic micelle-mediated reactions are believed to occur in this region). On the other hand, the presence of Ag^+ in this region cannot be ruled out completely, because the micellar Stern layer is water rich. CTAB micelles stabilize and/or solubilize the reactants into its small volume due to various interactions. A complete understanding of the micellar effect is not possible, because a number of different interactions, including those associated with the head group of the surfactant, are involved. The appearance and/or change of colour strongly depends on the presence of CTAB in the reaction mixture. The morphology of Ag nanoparticles can be controlled not only by the CTAB, but also by the alteration in reaction time. From these observations, it is clear that CTAB not only stabilized and/or capped the nanoparticles, but also altered the nucleation process. Thus, we may state confidently that the presence of suitable stabilizer(s) is essential for the appearance of prefect transparent stable silver sols.

The UV–Vis absorption spectrum of the resulting AgNPs prepared in the presence of sunlight using CTAB as stabilizer agent is shown in Fig. 2, which reveals the fast nucleation and/or reduction of Ag^+ ions into the metallic Ag^0 (nanoparticles) with surface plasmon absorption maxima at 450 nm. Comparison of Figs. 1 and 2 clearly suggests the catalytic role of sunlight which might be due to the presence of bioactive constituents of lemon. The position and shape of the plasmon absorption depends on the presence of sunlight. We can observe that surface plasmon absorption maximum initially at 460–475 nm is shifted to lower wavelength (Fig. 2) in the presence of sunlight. It has been established that the position of λ_{max} (blue and red shift) depends on the morphology of the resulting nanomaterials [47]. The blueshifting, probably due to the interparticle interaction and/or aggregation of water-soluble AgNPs in the presence of sunlight, suggests that the initially small AgNPs grow to form larger particles. Interestingly, our spectra do not show a tail extending into the red (Fig. 2), indicating that the resulting AgNPs have significant aggregation. As the reaction time increases, a new broad shoulder begins to develop in the vicinity of 650 nm, suggesting that particles have a wide size distribution in the presence of sunlight [48]. The appearance of this shoulder can be attributed to the multiplasmon excitation of faceted and anisotropic nanoparticles. Figure 3a–c shows the TEM images of nanoparticle solution along with the mean particle size. All the nanoparticles are spherical in shape; it can be seen that each particle is surrounded by a layer and are polydispersed. Inspection of TEM images clearly indicates that each particles is a bunch of a large number of triangular nanoplates (Fig. 3b; denoted by the red circle). Silver nanoplates (polyhedral shaped) were formed by the corner dissolution of triangular nanoparticles. All these particles fall in the size range of 4 to 39 nm. The particle size increases with [CTAB]. The corresponding particle size distribution histogram is given blow the spectra of Fig. 1b. Thus, we may safely conclude that CTAB acted as a shape-directing agent [15–17]. Henglein et al. [49] used a pulse radiolysis technique and discussed the mechanisms of AgNPs formation in aqueous ethanol solution. They suggested the three steps for the reduction of Ag^+ ions to Ag^0 atoms (Ag^+ (aq) + $e^- \rightarrow Ag^0$; $Ag^0 + Ag^+ \rightarrow Ag^{2+}$; $2Ag^{2+} \rightarrow Ag_4^{2+}$). The same elementary reactions were also considered by various researchers at different occasions [50]. Various species such as Ag_2^+, Ag_3^{2+}, Ag_4^{2+}, Ag_8Ag^+ or Ag_9^+ and Ag_6^{4+} exist in aqueous solution and in zeolites [49]. Out of these species, only Ag_4^{2+} can be stabilized for a long time in the presence of a polyanion even under air and growth stops at the stage of this species [6]. Interestingly, no turbid solution of AgCl was detected in the presence of NaCl. This result indicated

Table 1 Zone inhibition and minimum inhibitory concentration of AgNPs prepared by using lemon juice aqueous extract against gentamicin and two bacterial strains

Sample	Concentration (μg/ml)	Zone inhibition (mm)	
		E. coli (MTCC405)	*S. aureus* (MTCC3160)
AgNPs	5	–	9
	10	8	11
	15	10	14
	20	12	16
Gentamicin	5	14	22

	Minimum inhibitory concentration (MIC)	
	E. coli (MTCC405) (μg/ml)	*S. aureus* (MTCC3160) (μg/ml)
AgNPs	50	22.3
$AgNO_3$	80	120
Gentamicin	0.5–32	4–32

that essentially all Ag^+ ions have been converted into Ag^0 during the redox process and/or adsorbed on the surface of silver cluster, i.e., Ag_4^{2+}. Thus, we may safely conclude that Cl^- ions could not detach the adsorbed Ag^+ from the Ag_4^{2+}. It should be emphasized that the solutions were non-opalescent before as well as after the addition of Cl^- as viewed by the naked eye.

Antibacterial and antifungal activities of AgNPs

The combination effect of silver and their AgNPs solution with two different bacteria was investigated against *S. aureus* and *E. coli* using the disc diffusion method. The diameter of inhibition zones (in millimetres) around the different compounds discs with or without AgNPs against test strains are shown in Table 1. Figure 4 shows the % cell viability and disc plates to which a bacterial suspension (*E. coli* and *S. aureus*) was applied. In the case of *E. coli*, antibacterial activity decreases markedly with increasing concentration of AgNPs, while in the case of *S. aureus*, there are no considerable changes in cell viability after 50 µg/ml. The presence of nanoparticles at a certain level inhibited bacterial growth by more than 90 %. The diameter of inhibition zones (in millimetres) around the different silver nanoparticles sols against the test strain is shown in Table 1. Increase in [both strains] show a higher susceptibility. We observed that 80 % MIC at 31.25–50 µg/ml against *E. coli* (MTCC405) and 7.8–22.5 µg/ml against *S. aureus* (MTCC3160). However, it is necessary to determine the minimum inhibitory concentration (MIC). Figure 4 also shows the antibacterial potential of AgNPs which were found to be highly toxic towards *S. aureus* in comparison to *E. coli* and their cell viability was less than 50 %. The antibacterial activities increased in the presence of AgNPs solution against both test strains. The highest fold increases in area were observed in the presence of AgNPs against *S. aureus*. It is clear that the growth of the bacterial colonies around the AgNPs is inhibited (Fig. 4), whereas a dense population of bacterial colonies appear in the control set that contains pieces of plain fabric in the Petri dish (Fig. 4). The observed inhibiting action of AgNPs might be due to the release of Ag^+ ions from AgNPs. These Ag^+ ions come in contact with bacterial cells and kill them. The antifungal activities of AgNPs increased with increasing the concentrations of AgNPs against all three species of *Candida* fungus (Table 2). The highest fold increases in area were observed for *C. albicans* (Fig. 5). The action of lemon-assisted AgNPs fungi is perhaps even more dramatic. Our study showed that the growth of all fungi was totally inhibited by an aqueous solution of AgNPs. Medically important fungi and yeasts (notably *C. albicans* are also inhibited and then killed by increasing concentrations).

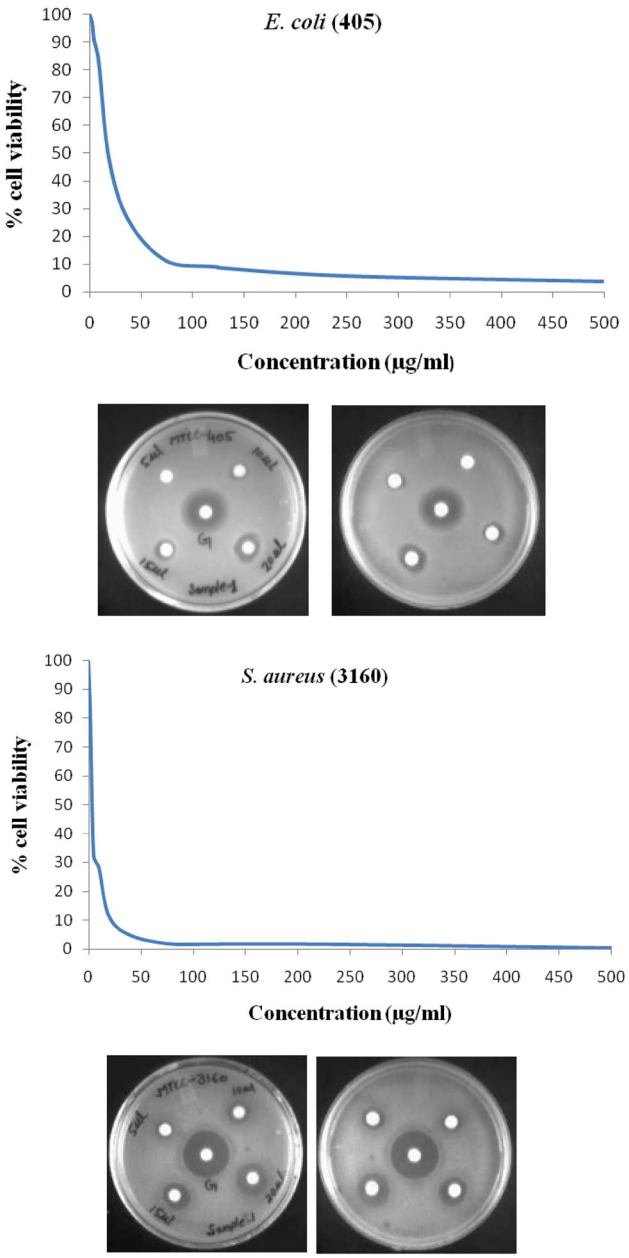

Fig. 4 Cell viability and disc diffusion assay of AgNPs against *E. coli* (MTCC405) and *S. aureus* (MTCC3160)

AgNPs show efficient antibacterial and antifungal property due to their extremely large surface area, which provides better contact with microorganisms and breaks down the membrane permeability barrier of *Candida* fungus (membrane lipid bilayers changed), forming pores and dissipating the electrical potential of the membrane [51].

Mechanism of inhibitory action

It has been established that the mechanism of inhibitory action of Ag^+ ions and its nanomaterials on microorganisms would be due to the electrostatic interaction

Table 2 Zone inhibition and minimum inhibitory concentrations (MIC) of AgNPs prepared by using lemon juice aqueous extract against fluconazole and three species of *Candida* fungus

Sample	Concentration (μg/ml)	Zone inhibition (mm)		
		C. albicans (ATCC90028)	*C. tropicalis* (ATCC750)	*C. glabrata* (ATCC90030)
AgNPs	5	5	10	11
	10	7	15	13
	15	9	17	15
Fluconazole	5	20	14	28

	Minimum inhibitory concentration (MIC)		
	C. albicans (ATCC90028) (μg/ml)	*C. tropicalis* (ATCC750) (μg/ml)	*C. glabrata* (ATCC90030) (μg/ml)
AgNPs	40–60	15–20	8–15
$AgNO_3$	60–100	60–100	60–100
Fluconazole	0.5–32	4–32	5–32

Scheme 2 Inhibitory action of bacterial cell membrane by AgNPs

$$(Ag)_n^+ + (\text{HS-cell membrane})_n \underset{}{\overset{K_{eq}}{\rightleftharpoons}} (\text{Ag-HS-cell membrane})_n^+ \quad (1)$$

$$(\text{Ag-HS-cell membrane})_n^+ \xrightarrow{K} Ag^+ + (\dot{S}\text{-cell membrane})_n + (Ag)_{n-1} \quad (2)$$

$$(\dot{S}\text{-cell membrane})_n \xrightarrow{\text{Fast, dimerization}} \text{Cysteine containing cell membrane} \quad (3)$$

(complexation and/or attached with cell membrane) between the Ag^+ ions and/or its nanoparticles with the DNA, cellular proteins, sulphur-containing (especially thiol group) functional groups of respiratory enzymes or proteins, negatively charged bacterial cells and building elements of the bacterial membrane. As a result, DNA loses replication ability, silver nanoparticles penetrate inside the bacteria, causes protein inactivation, denaturation, structural changes and degradation, inhibits the respiration process and finally causes cell death [52–55]. Sondi and Salopek-Sondi also suggested that the AgNPs release silver ions in the bacterial cells, which enhance their bactericidal activity [52]. Cysteine is a sulphur-containing α- amino acid (one of the monomers of the polymer proteins and/or enzyme). The thiol side chain in cysteine often participates in enzymatic reactions, serving as a nucleophile. The thiol group is susceptible to oxidation to give the disulphide derivative cysteine, which serves an important structural role in many proteins. Side chains (HS–) of cysteine possess high affinities towards Ag^+ ions (sulphur has been established as the most susceptible to gain electrons from oxidizing agents). On the basis of the previous discussion and thiol group properties of cysteine, we assumed that inhibitory action of bacteria might be due to the reduction of the HS cell membrane by AgNPs (Scheme 2).

In Scheme 2, the thiol groups of cell membrane protein form an ion pair between the positive surface of AgNPs, i.e., $(Ag)_n$ and lone electron pairs of sulphur atom of cysteine. By analogy with the previous results [56], we assume that the ion pair complex undergoes one-step oxidation–reduction mechanism, leadings to the formation of the cysteinyl radical (Eq. 2). The radical is unstable and immediately gets converted into a stable oxidation product of cysteine, i.e., cysteine (Eq. 3). The proposed mechanism is in good agreement with the suggestions of Sondi and Salopek-Sondi [52] regarding the release of Ag^+ ions in the bacteria cell which are responsible for the structural changes in the protein of the cell wall and one of the reasons for cell death and the picosecond dynamics and fragmentation of silver nanoclusters [57].

Conclusions

The silver nanoparticles produced by the lemon aqueous extract reduction method in the presence of CTAB was found to be stable, and sunlight acted as a catalyst during the nucleation processes. This method can give highly stable nanoparticles with different ratios of CTAB. Their antimicrobial activities were tested against Gram-positive bacteria *S. aureus* and Gram-negative bacteria *E. coli.* AgNPs have significant activity towards *S. aureus* in comparison to *E. coli*. This is the first report concerning the activity of gentamicin and fluconazole against two bacteria stains and three species of *Candida* fungus by Ag-NPs synthesized using lemon juice extract. The SH group of bacteria cell membrane is damaged by the AgNPs which causes the structural changes in the cell wall. AgNPs show

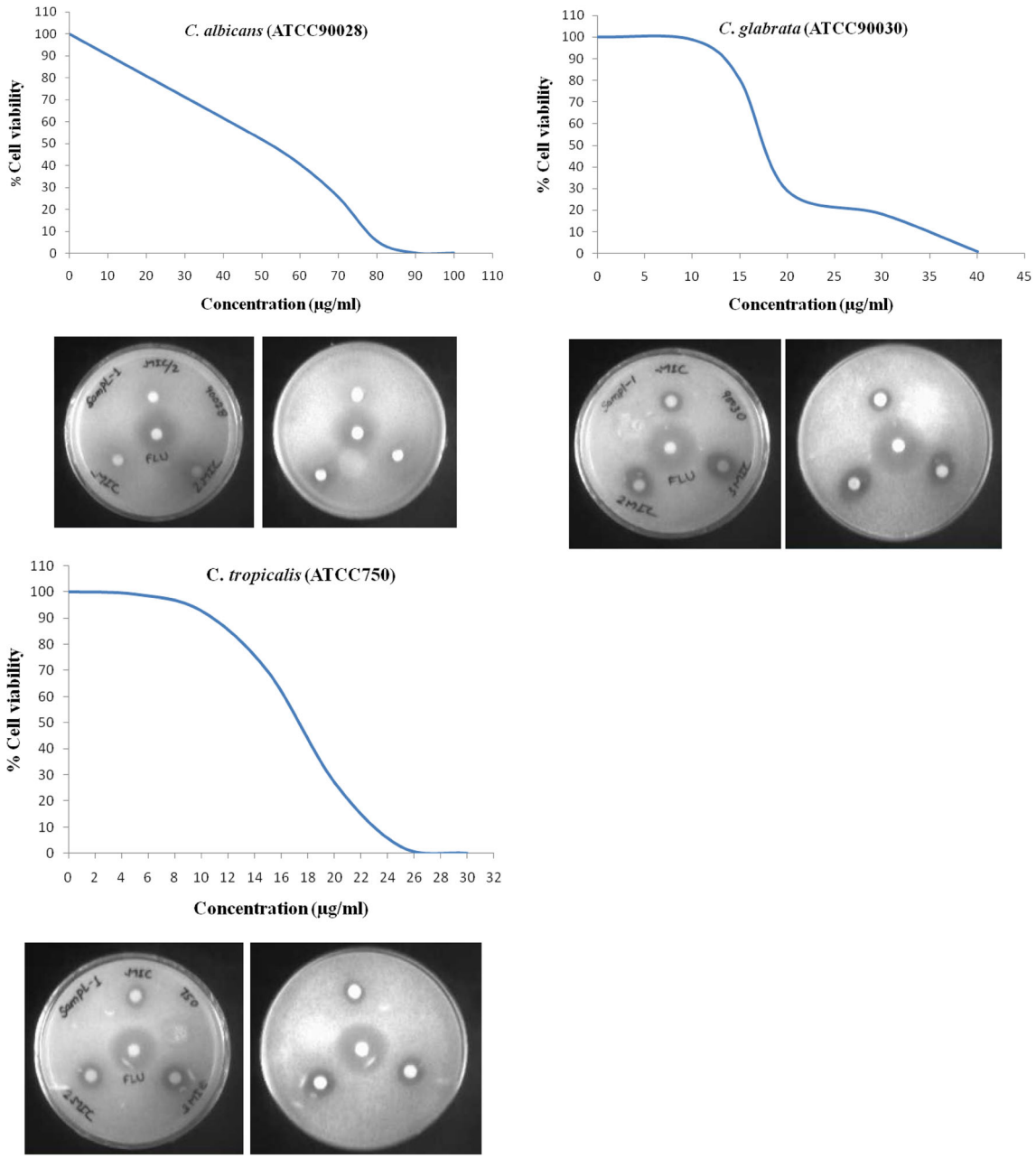

Fig. 5 Cell viability and disc diffusion assay of AgNPs against fungus *C. albicans* (ATCC90028), *C. tropicalis* (ATCC750) and *C. glabrata* (ATCC90030)

great potential towards *E. coli*, *S. aureus* and *Candida* species, which could be used as an antiseptic dressing or bandage in future for biomedical applications due to their high demand.

References

1. Clement JL, Jarrett PL (1994) Met-Based Drugs 1(5–6):467–482
2. Lansdown, Alan BG (2010) Silver in healthcare: Its antimicrobial efficacy and safety in use. Royal Soc Chem 159, ISBN 1-84973-006-7
3. Geranio L, Heuberger M, Nowack B (2009) Environ Sci Technol 43:8113–8118
4. Maillard JY, Hartemann P (2013) Crit Rev Microbiol 39:373–383
5. Johnston HJ, Hutchison G, Christensen FM, Peters S, Hankin S, Stone V (2010) Crit Rev Toxicol 40(4):328–346
6. Rai M, Yadav A, Gade A (2009) Biotechnology Adv 27:76–83
7. Fendler JH (1987) Chem Rev 87:877–899
8. Henglein A (1993) J Phys Chem 97:5457–5471
9. Sun Y, Mayers B, Xia Y (2003) Nano Lett 3(5):675–679
10. Yu D, Yam VW (2004) J Am Chem Soc 126:13200–13201
11. Burda C, Chen X, Narayanan R, El-Sayed MA (2005) Chem Rev 105:1025–1102
12. Dreaden EC, Alkilany AM, Huang X, Murphy CJ, El-Sayed MA (2012) Chem Soc Rev 41:2740–2779

13. Lu H, Zhang H, Yu X, Zeng S, Yong KT, Ho HP (2012) Plasmonics 7:167–173
14. Sinha AK, Basu M, Sarkar S, Pradhan M, Pal T (2013) J Colloid Interf Sci 398:13–21
15. Singh A, Kaur S, Kaur A, Aree T, Kaur N, Singh N, Bakshi MS (2014) ACS Sustainable. Chem Eng 2:982–990
16. Bakshi MS (2011) J Phys Chem 115:13947–13960
17. Sun Y, Xia Y (2002) Science 298:2176–2179
18. Khan Z, Al-Thabaiti SA, Obaid AY, Khan ZA, Al-Youbi AO (2012) J Colloid Interf Sci 367:101–108
19. Khan Z, AL-Thabaiti SA, El-Mossalamy EH, Obaid AY (2013) Mater Res Bull 48:1137–1143
20. Hussain S, Akrema, Rahisuddin, Khan Z (2014) Bioproc Biosyst Eng 37:953–964
21. Bashir O, Hussain S, Al-Thabaiti SA, Khan Z (2014) Carbohyd Polym 107:167–173
22. Yu D, Yam VWW (2004) J Am Chem Soc 126(2004):13200–13201
23. Feng QL, Wu J, Chen GQ, Cui FZ, Kim TN, Kim JO (2000) J Biomed Mater Res 52:662–668
24. Brigger I, Dubernet C, Couvreur P (2004) Adv Drug Deliver Rev 54:6310
25. Song HY, Ko KK, Oh IH, Lee BT (2006) Eur Cells Mater 11:58
26. Shahverdi AR, Fakhimi A, Shahverdi HR, Minaian MS (2007) Nanomedicine 3:168–171
27. Guzman MG, Dille J, Godet S (2009) Int J Chem Biol Eng 2:104–111
28. Sharma VK, Yngard RA, Lin Y (2009) Adv Colloid Interf Sci 145:83–96
29. Dong PV, Ha CH, Binh LT, Kasbohm J (2012) Int Nano Lett 2:9
30. Shankar SS, Rai A, Ahmad A, Sastry M (2004) J Colloid Interf Sci 275:496–502
31. Khan Z, Hussain JI, Hashmi AA (2012) Colloid Surface B 98:85–90
32. Hussain S, Khan Z (2014) Bioproc Biosyst Eng 37:1221–1231
33. Vandercook CE, Stephenson RG (1966) J Agric Food Chem 14:450–454
34. Okwi DE, Emenike IN (2006) International J Mol Med Ad Sci 2:1–6
35. Okwu DE, Emenike IN (2007) J Food Technology 5:105–108
36. Garcia OB, Castillo J, Marin JR, Ortuno A, Del Rio JA (1997) J Agric Food Chem 45:4505–4515
37. Vinson JA, Su X, Zubik L, Bose P (2001) J Agric Food Chem 49:5315–5321
38. Penniston KL, Nakada SY, Holmes RP, Assimos DG (2008) J Endourolo 22:567–570
39. Prathna TC, Chandrasekaran N, Raichur AM, Mukherjee A (2011) Colloid Surface B 82:152–159
40. Prathna TC, Raichur AM, Chandrasekaran N, Mukherjee A (2014) Proc Natl Acad Sci India B Biol Sci 84:65–70
41. Vankar PS, Shukla D (2012) Appl Nanosci 2:163–168
42. Nisha NS, Aysha OS, Rahaman SNJ, Kumar VP, Valli S, Nirmal P, Reen A (2014) Spcetrochim Acta A Mol Biomol Spectrosc 124:194–201
43. Hussain S, Al-Thabaiti SA, Khan Z (2014) Bioprocess Biosyst Eng 37:1727–1735
44. Sigmann SB, Wheeler DE (2004) J Chem Ed 81:1479–1481
45. Pal S, Kyung Y, Song JM (2007) App Env Microbiol 73:1712–1720
46. Jin R, Cho YW, Markin CA, Kelly KL, Schatz GC, Zheng JG (2001) Science 294:1901–1903
47. Linnert T, Mulvaney P, Hanglein A, Weller H (1990) J Am Chem Soc 112:4657–4664
48. Song JY, Kim BS (2009) Bioprocess Biosyst Eng 32:79–84
49. Ershov BG, Henglein A (1998) J Phys Chem B 102:10663–10666
50. Mostafavi M, Dey GR, François L, Belloni J (2002) J Phys Chem A 106:10184–10194
51. Keuk-Jun K, Woo SS, Bo KS, Seok-Ki M, Jong-Soo C, Jong GK, Dong GL (2009) Biometals 22:235–242
52. Sondi I, Salopek-Sondi B (2004) J Colloid Interf Sci 275:177–182
53. Ales PC, Milan K, Renata V, Robert P, Jana S, Vladimir K, Petr H, Radek Z, Libor K (2009) Biomaterials 30:6333–6340
54. Rai M, Yadav A, Gade A (2009) Biotechnol Adv 27:76–83
55. Klasen HJ (2000) Burns 30:1–9
56. Khan Z, Talib A (2010) Colloid Surface B 76:164–169
57. Kamat PV, Flumiani M, Hartland GV (1998) J Phys Chem B 102:3123–3128